buoyant effect. Secondly the interfacial shear is smaller and in many instances the shear force acts in the opposite direction compared with the Freon 12–nitrogen mixture (see Table 1 for $f_V''(0)$). Furthermore the fact that the buoyant effect introduces a larger shear force at the interface for the case of Freon 12–nitrogen mixture may promote instability in both the vapor boundary layer and the liquid–vapor interface as pointed out by the experimental work of Spencer et al. [7]. They observed the instability of the vapor boundary layer while operating on a saturated bulk temperature from 80 to 100°F and a temperature difference between the bulk and the wall being about 2–36°F with a mass fraction of the condensable vapor in the bulk form 0·993 or less. Two heat-transfer results are shown in Fig. 2. It is seen that the presence of a small amount of noncondensable gas in the bulk may cause a considerable reduction in heat transfer such that a presence of 0·01 per cent of nitrogen in Freon 12 vapor operating at 0°F may cause a reduction in heat transfer more than 10 per cent. It is noted that as the pressure (temperature) at which condensation process takes place decreases, the effect of noncondensable gas in reducing heat transfer increases. This trend is observed in steam–air system studied by Minkowycz and Sparrow [5]. Physically, when the operating pressure (temperature) decreases, the mixture density decreases. Therefore, the ratio of $(\rho\mu)_L/(\rho\mu)_V$ increases. As a consequence, the interfacial concentration of noncondensable gas increases and thus causes a reduction in heat transfer. In general, in the case of Freon 12–nitrogen mixture, numerical results show that the temperature drop in the liquid phase is more pronounced than that in the vapor phase. For example (Table 2), when the operating temperature, $T_\infty$, is at 48·1°F with $Sc = 0·3$, $W_{1\infty} = 0·9999$, we obtain $T_i = 46·3°F$ when $T_w = 16·6°F$. On the contrary, the trend is generally opposite in the case of steam–air mixture.

As an example [8], we have $T_\infty = 200°F$ with $Sc = 0·5$, $W_{1\infty} = 0·98$ then $T_i = 180·8°F$ when $T_w = 177·3°F$. It should be remarked finally that similarity solution does not exist for high bulk concentration of noncondensable gas in the case of lighter noncondensable.

### REFERENCES

1. H. Hampson, Proceedings of the General Discussion on Heat Transfer, Vol. 84, pp. 58–61. Institution of Mechanical Engineers, London, and American Society of Mechanical Engineers, New York (1951).
2. L. Slegers and R. A. Seban, Laminar film condensation of steam containing small concentrations of air, Int. J. Heat Mass Transfer 13, 1941–1946 (1970).
3. H. K. Al-Diwany and J. W. Rose, Free convection film condensation of steam in the presence of non-condensing gases, Int. J. Heat Mass Transfer 16, 1359–1369 (1973).
4. E. M. Sparrow and S. H. Lin, Condensation heat transfer in the presence of a noncondensable gas, J. Heat Transfer 86, 430–436 (1964).
5. W. J. Minkowycz and E. M. Sparrow, Condensation heat transfer in the presence of noncondensable, interfacial resistance, superheating, variable properties and diffusion, Int. J. Heat Mass Transfer 9, 1125–1144 (1966).
6. J. W. Rose, Condensation of a vapour in the presence of a non-condensing gas, Int. J. Heat Mass Transfer 12, 233–237 (1969).
7. D. L. Spencer, K. I. Chang and H. C. Moy, Experimental investigation of stability effects in laminar film condensation on a vertical cylinder, Heat Transfer 1970, Vol. 6, Chapter 2.3, pp. 1–11 (1970).
8. O. Rutunaprakarn, Effects of noncondensable gas with different molecular weight on laminar film condensation, M. S. Thesis, Department of Mechanical Engineering, The University of Iowa (May 1973).

# GRAETZ PROBLEM IN CURVED RECTANGULAR CHANNELS WITH CONVECTIVE BOUNDARY CONDITION—THE EFFECT OF SECONDARY FLOW ON LIQUID SOLIDIFICATION-FREE ZONE

K. C. CHENG, RAN-CHAU LIN and JENN-WUU OU
Department of Mechanical Engineering, University of Alberta, Edmonton, Alberta, Canada

### NOMENCLATURE

$Bi$, Biot number, $hD_e/k$;
$D_e$, equivalent hydraulic diameter, $2ab/(a+b)$;
$h$, heat-transfer coefficient, $-k(\partial T/\partial N)_w = h(T_w - T_\infty)$;
$K$, Dean number, $Re(D_e/R)^{1/2}$;
$k$, thermal conductivity;
$N$, outward normal at wall;
$Nu$, local Nusselt number, $\bar{h}D_e/k$;
$n$, dimensionless outward normal, $N/D_e$;
$Pr$, Prandtl number, $v/\alpha$;
$R$, radius of curvature;
$Re$, Reynolds number, $D_e \bar{W}/v$;
$r$, dimensionless radius of curvature, $R/D_e$;
$T, T_f, T_0, T_\infty$, fluid temperature, freezing temperature of liquid, uniform fluid entrance temperature and ambient fluid temperature, respectively;
$U, V, W$, velocity components in $X, Y, Z$ directions;

$\bar{W}$, average axial velocity;
$u, v, w$, dimensionless velocity components, $[(U, V)/(v/D_e), W/\bar{W}]$;
$X, Y, Z$, Cartesian coordinates;
$x, y, z$, dimensionless coordinates, $[(X, Y)/D_e, Z/D_e(PrRe)]$;
$z_f$, dimensionless entrance distance where solidification begins;
$\gamma$, aspect ratio of a rectangular channel, $b/a$;
$\varepsilon$, superheat ratio, $(T_0 - T_f)/(T_f - T_\infty)$;
$\theta$, dimensionless temperature difference, $(T - T_\infty)/(T_0 - T_\infty)$;
$\theta_b, \theta_w$, bulk temperature,

$$\iint_A \theta w \, dx \, dy \bigg/ \iint_A w \, dx \, dy,$$

and local wall temperature;
$\psi$, dimensionless stream function [12, 13];
$\bar{\phantom{x}}$, average quantity.

## 1. INTRODUCTION

THE AVAILABLE solutions [1–6] to Graetz problems with convective boundary condition are fairly limited and are so far confined to straight tubes and parallel-plate channels only. The convective boundary condition is of practical importance since such effects as wall resistance, thermal insulation and external surface resistance can be accommodated. Furthermore, the limiting cases lead to the constant wall temperature ($Bi = \infty$) and the perfectly insulated case ($Bi = 0$), respectively. Thus, for most practical cases, the Biot number has a finite value.

Recently, the Graetz problem in curved circular pipes has been studied by several investigators [7–11]. However, these investigations have been concerned with the thermal boundary condition of constant wall temperature or uniform wall heat flux only. It appears that no investigation has been reported for the Graetz problem in curved pipes or channels with the convective boundary condition in spite of its practical and theoretical importance.

The purpose of this paper is to study the effects of convective boundary condition on thermal entrance region heat-transfer characteristics and the effect of secondary flow on liquid solidification-free zone in curved rectangular channels.

It should be pointed out that the solidification of the liquids flowing in curved tubes or channels may occur under extreme ambient conditions. In practice, the external heat-transfer coefficient may vary circumferentially or axially.

## 2. ANALYSIS

Consider a steady fully developed laminar incompressible flow in a curved rectangular channel where at the channel section $Z = 0$ a uniform cooling begins. Using the toroidal coordinate system shown in Fig. 1, the energy equation in dimensionless form becomes [12, 13].

$$u\frac{\partial \theta}{\partial x} + v\frac{\partial \theta}{\partial y} + \frac{w}{1+(x/r)}\frac{1}{Pr}\frac{\partial \theta}{\partial z}$$
$$= \frac{1}{Pr}\left[\frac{\partial^2 \theta}{\partial x^2} + \frac{\partial^2 \theta}{\partial y^2} + \frac{1}{r(1+x/r)}\frac{\partial \theta}{\partial x}\right] \quad (1)$$

$$\theta = 1 \text{ at } z \leqslant 0, \quad \partial\theta/\partial n = -Bi\theta_w \text{ at wall,}$$
$$\partial\theta/\partial y = 0 \text{ along } y = 0. \quad (2)$$

It is noted that Dean's original formulation for the curved pipe corresponds to the case with $1/r = 0$. The numerical solution of the complete Navier–Stokes equations for the flow problem in curved rectangular channels considering the curvature ratio effect in the analysis is given in [12, 13] and the numerical results are utilized in this study. The numerical solution reveals that at a certain higher Dean number an additional pair of counter-rotating vortex rolls appears near the central outer region of the curved channel as shown in Fig. 1. The present hydrodynamic instability phenomenon is consistent with Dean's centrifugal instability problem [14] in a curved parallel-plate channel flow and the instability is found to occur already at Dean number $K = 202$ with the curvature ratio $r = 100$ in a curved square channel [12, 13]. The local Nusselt number, $hD_e/k$, can be evaluated by considering either the local wall temperature gradient or an overall energy balance as,

$$Nu_1 = Bi\theta_w/(\theta_b - \theta_w), \quad Nu_2 = \frac{-1}{4(\theta_b - \theta_w)}\left(\frac{w}{1+x/r}\frac{\partial \theta}{\partial z}\right). \quad (3)$$

Equations (1) and (2) are solved by a finite-difference procedure using Peaceman and Rachford's alternating direction implicit (ADI) method and a complete account of the numerical analysis is presented in [13]. The mesh size ($M \times N$) used is similar to that used in fully developed flow problem [12, 13]. For example, the mesh sizes of $20 \times 10$ and $40 \times 20$ for higher Dean numbers are found to be satisfactory from the viewpoint of accuracy and computing time for curved square channel.

In the case of the curved square channel, the two Nusselt
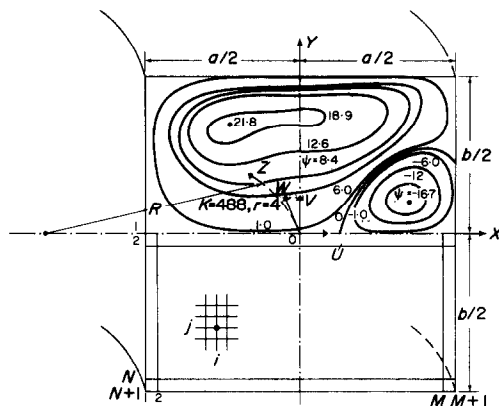


FIG. 1. Coordinate system for a curved square channel and secondary flow pattern at $K = 488$ and $r = 4$.
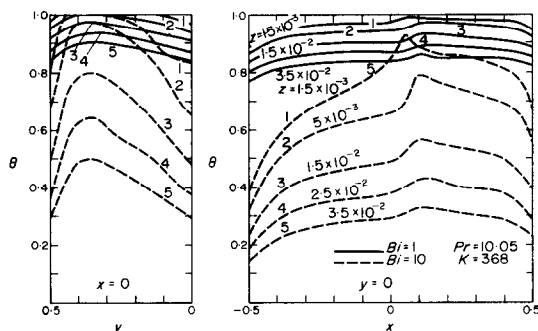


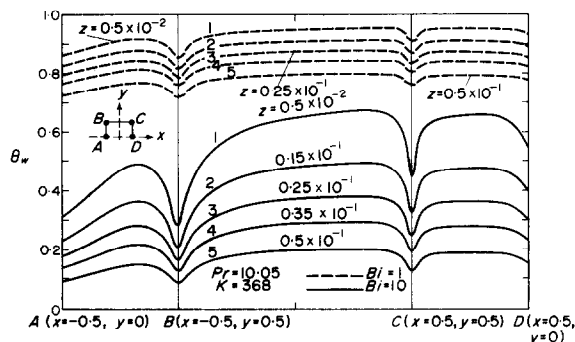FIG. 2. Temperature profile development at $x = 0$ and $y = 0$ for $Pr = 10.05$, $K = 368$ with $Bi = 1$ and 10.



FIG. 3. Development of peripheral wall temperature distribution for $Pr = 10.05$, $K = 368$ with $Bi = 1$ and 10.

number values, $Nu_1$ and $Nu_2$ agree to within 1 per cent, for example for $Pr = 10.05$, $K = 488$ with Biot numbers 1 and 10. At $K = 0$ and $Bi = 10$, the asymptotic Nusselt number of 2.985 also agrees excellently with the value of 2.988 for the case of uniform wall temperature ($Bi \to \infty$). Thus, one may conclude that the convergence and accuracy of the numerical solution are satisfactory.

## 3. HEAT-TRANSFER RESULTS

### 3.1. Temperature field development

The development of the temperature field along the central horizontal and vertical planes of a curved square channel is shown in Fig. 2 for $Pr = 10.05$, $K = 368$ and $Bi = 1, 10$. The corresponding wall temperature distribution $\theta_w$ around the channel periphery is shown in Fig. 3. It is noted that at $K = 368$, an additional pair of vortex rolls already appears near the central outer region of the channel. Because of the nature of the present convective boundary condition, the developing wall temperature distribution for $\theta_w$ is of special
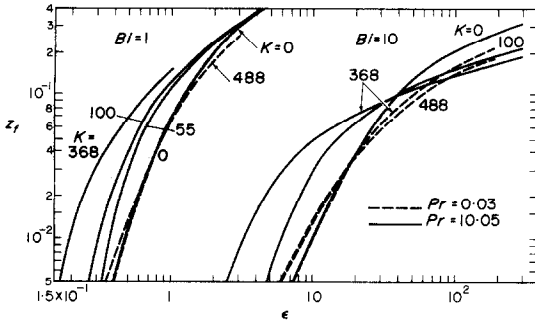
FIG. 4. Length of liquid solidification-free zone for $Pr = 0.03, 10.05$ and $Bi = 1, 10$ with $K$ as parameter.
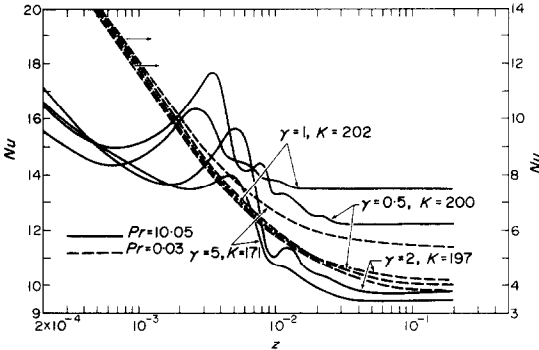


FIG. 5. Local Nusselt number variation for $Pr = 0.03, 10.05$ and $Bi = 10$ in curved rectangular channels with aspect ratios $\gamma = 1, 2, 5, 0.5$.

interest. It is clearly seen that the value of $\theta_w$ is lowest at the inside corners. It should be pointed out that the secondary flow is rather weak near the corners. Noting the relationship $\partial\theta/\partial n = -Bi\theta_w$ from equation (2) and the fact that the Biot number is constant, it is seen that the distribution of the wall temperature gradient $\partial\theta/\partial n$ is also similar to the distribution for $\theta_w$.

### 3.2. Local Nusselt number result

The effects of the Dean and Prandtl numbers on the local Nusselt number behaviour in the thermal entrance region of the curved square channel are studied in [13]. The Biot number effect on the local Nusselt number is found to be rather small. The asymptotic Nusselt number is of practical interest and the results for square channels are given in Table 1.

Table 1. Asymptotic Nusselt number

| $Pr$ | $K$ | $Nu_f$ | | |
| | | $Bi = 1$ | $Bi = 10$ | $Bi = \infty$ |
| --- | --- | --- | --- | --- |
| — | 0 | 3.009 | 2.985 | 2.98 |
| 0.7 | 100 | 6.051 | 6.023 | 6.000 |
| | 368 | 11.340 | 11.000 | 10.760 |
| 10.05 | 55 | 7.003 | 6.799 | 6.793 |
| | 100 | 8.323 | 8.127 | 8.018 |
| | 368 | 16.836 | 16.390 | 16.031 |

It is noted that the Biot number effect is rather small and a maximum deviation from the uniform wall temperature case $(Bi \to \infty)$ is only 4 per cent for a given Dean number. Both the Prandtl and Dean numbers have the effect of decreasing the thermal entrance length [13].

The curvature ratio effect is included in the analysis as an independent parameter. However, based on recent investigations [15, 16] for fully developed laminar heat transfer in
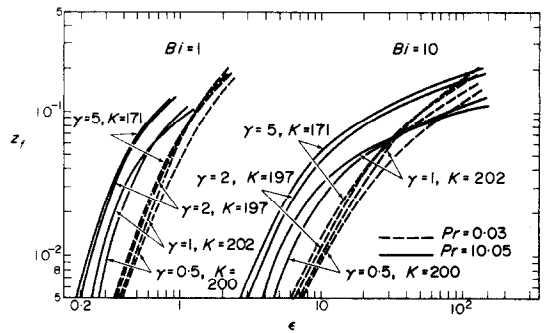


FIG. 6. Length of liquid solidification-free zone for $Pr = 0.03, 10.05$ and $Bi = 1, 10$ in curved rectangular channels with aspect ratios $\gamma = 1, 2, 5, 0.5$.

curved pipes, it may be concluded that for $r \gtrsim 10$, the curvature ratio parameter has a negligible effect on local Nusselt number.

### 3.3. The effect of secondary flow on liquid solidification-free zone

In the case of uniform convective cooling at the outer surface with an ambient temperature $T_\infty$ lower than the liquid freezing temperature $T_f$ and in view of the wall temperature distribution $\theta_w$ shown in Fig. 3, it is clear that the liquid solidification will start at the inner corner point $B$ (Fig. 3) when the freezing temperature is reached there at some downstream distance referred to as the length of solidification-free zone or the solid-phase entrance $(z = z_f)$. When the solid-phase surrounds the channel inner wall completely, the thermal boundary condition for the liquid becomes an isothermal one. One may also reason that the solidification will start at the inner wall for the case of curved circular tubes. The solidification of the liquid metal or water in curved channels is of considerable practical importance. Apparently, the theoretical analysis on the liquid solidification problem [4, 5] in a curved tube or channel is not yet available in the literature.

For a study of the liquid solidification-free zone, it is convenient to introduce the superheat ratio parameter [4] defined as $\varepsilon = (T_0 - T_f)/(T_f - T_\infty) = -1 + \theta_f^{-1}$, where $\theta_f < 1$. It is noted that solidification begins when the wall temperature $\theta_w$ at inner corners (cold spot) equals $\theta_f$. Consequently, the superheat ratio $\varepsilon$ corresponding to the solidification-free length $z_f$ can be computed readily. The results for $\gamma = 1$ are plotted in Fig. 4 for $Pr = 0.03$ (liquid metal) and $10.05$ (water) with Dean number as parameter for the cases $Bi = 1$ and 10. Since the present analysis is based on the constant physical property assumption, with $Pr = 10$ for water, for example, the temperature difference $(T_0 - T_f)$ is practically limited to about 20°C. Furthermore, with $T_\infty = -0.5°C$ and $-100°C$, $\varepsilon$ becomes 40 and 0.2, respectively. In interpreting the results shown in Fig. 4, it is well to note that as $\varepsilon$ approaches zero and infinity, $z_f$ also approaches zero and infinity, respectively. The trend for $K = 0$ is similar to that reported in [4, 6] for straight tubes. With $Pr = 0.03$ and $Bi = 1$, the secondary flow effect seems to be small. It is sufficient here to use the case of $Pr = 10.05$ and $Bi = 10$ to explain the secondary flow effect on solidification-free zone. Apparently, the character of the Dean number effect changes at the threshold value of $\varepsilon \approx 37$. Noting that the value of $\varepsilon$ decreases as the ambient temperature $T_\infty$ decreases, with a given $\varepsilon < 37$, the secondary flow tends to mix the warmer liquid and correspondingly, the solidification-free length increases with the increase of Dean number. On the other hand, with $\varepsilon > 37$ (or relatively higher $T_\infty$) the secondary flow tends to bring the cold spot temperature to the freezing temperature at a shorter entrance distance $z_f$. Further physical insight can be gained by considering a given value of $z_f$ and the corresponding different values for the different Dean numbers.

For a given value of Biot number, the secondary flow effect on the length $z_f$ of liquid solidification-free zone is greater for larger Prandtl number. For given values of Prandtl number and superheat ratio, the Dean number effect on solidification-free length is completely opposite depending on whether the solidification occurs in thermally developing or fully developed zone.

### 3.4. Aspect ratio effect

The results for the typical local Nusselt number and solidification free zone for $Pr = 10.05$ (water) and $0.03$ (liquid metal) are presented in Figs. 5 and 6, respectively, for aspect ratios $\gamma = 1, 2, 5$ and $0.5$ with $Bi = 1$ and $10$. The Nusselt number behavior is characteristically different between $Pr = 0.03$ and $10.05$. The fluctuating Nusselt number phenomenon before approaching the asymptotic value for $Pr = 10.05$ and $K > 171$ is somewhat similar to the earlier investigations [7, 8, 11] but the number of fluctuating cycles before the complete damping is far fewer than that shown in Fig. 9 of [8] for the constant wall temperature case with $Pr = 10$ in helical coils. The aspect ratio effect can only be seen clearly with the comparable Dean numbers.

### REFERENCES

1. P. J. Schneider, Effect of axial fluid conduction on heat transfer in the entrance regions of parallel plates and tubes, *Trans. Am. Soc. Mech. Engrs* **79**, 765–773 (1957).
2. C. J. Hsu and C. J. Huang, Heat or mass transfer in laminar flow through a concentric annulus with convective flux at walls, *Chem. Engng Sci.* **21**, 209–221 (1966).
3. C. J. Hsu, Exact solution to entry-region laminar heat transfer with axial conduction and the boundary condition of the third kind, *Chem. Engng Sci.* **23**, 457–468 (1968).
4. G. S. H. Lock, R. D. J. Freeborn and R. H. Nyren, Analysis of ice formation in a convectively-cooled pipe, in *Heat Transfer*, Vol. 1, Cu 2.9. Elsevier, Amsterdam (1970).
5. R. D. Zerkle, The effect of external thermal insulation on liquid solidification in a tube, in *Proc. of 6th Southeastern Seminar on Thermal Sciences*, pp. 1–19 (1970).
6. G. J. Hwang and I. Yih, Correction on the length of ice-free zone in a convectively-cooled pipe, *Int. J. Heat Mass Transfer* **16**, 681–683 (1973).
7. A. N. Dravid, K. A. Smith, E. W. Merrill and P. L. T. Brian, Effect of secondary fluid motion on laminar flow heat transfer in helically coiled tubes, *A.I.Ch.E. Jl* **17**, 1114–1122 (1971).
8. J. M. Tarbell and M. R. Samuels, Momentum and heat transfer in helical coils, *Chem. Engng Jl* **5**, 117–127 (1973).
9. M. Akiyama and K. C. Cheng, Laminar forced convection in the thermal entrance region of curved pipes with uniform wall temperature, *Can. J. Chem. Engng* **52**, 234–240 (1974).
10. M. Akiyama and K. C. Cheng, Graetz problem in curved pipes with uniform wall heat flux, *Appl. Scient. Res.* In press.
11. S. V. Patankar, V. S. Pratap and D. B. Spalding, Prediction of laminar flow and heat transfer in helically coiled pipes, *J. Fluid Mech.* **62**, 539–551 (1974).
12. K. C. Cheng, R. C. Lin and J. W. Ou, Fully developed laminar flow in curved rectangular channels, *J. Fluids Engng.* In press.
13. R. C. Lin, Fully developed laminar flow and Graetz problem in curved rectangular channels, M.Sc. thesis, Mechanical Engineering Department, University of Alberta, Edmonton, Alberta, Canada (1974).
14. J. T. Stuart, Hydrodynamic stability, in *Laminar Boundary Layers* (edited by L. Rosenhead), p. 505. Oxford University Press, Oxford (1963).
15. C. E. Kalb and J. D. Seader, Heat and mass transfer phenomena for viscous flow in curved circular tubes, *Int. J. Heat Mass Transfer* **15**, 801–817 (1972).
16. C. E. Kalb and J. D. Seader, Fully developed viscous-flow heat transfer in curved circular tubes with uniform wall temperature, *A.I.Ch.E. Jl* **20**, 340–346 (1974).